J|A|C|S
ARTICLES
Published on Web 06/20/2006

U(SMes*)$_n$, (n = 3, 4) and Ln(SMes*)$_3$ (Ln = La, Ce, Pr, Nd): Lanthanide(III)/Actinide(III) Differentiation in Agostic Interactions and an Unprecedented η^3 Ligation Mode of the Arylthiolate Ligand, from X-ray Diffraction and DFT Analysis

Mathieu Roger,[†] Noémi Barros,[‡] Thérèse Arliguie,*[,†] Pierre Thuéry,[†] Laurent Maron,*[,§] and Michel Ephritikhine*[,†]

Contribution from the Service de Chimie Moléculaire, DSM, DRECAM, CNRS URA 331, CEA/Saclay, 91191 Gif-sur-Yvette, France, Service de Chimie des Procédés de Séparation, DEN, DRCP, CEA/Valrhô, BP 17171, 30207 Bagnols-sur-Cèze, France, and Laboratoire de Physique Quantique, IRSAMC, CNRS UMR 5626, Université Paul Sabatier, 118 route de Narbonne, 31062 Toulouse Cedex, France

Received December 22, 2005; E-mail: therese.arliguie@cea.fr

Abstract: Reaction of U(NEt$_2$)$_4$ with HS-2,4,6-^{t}Bu$_3$C$_6$H$_2$ (HSMes*) gave U(SMes*)$_3$(NEt$_2$)(py) (**1**), whereas similar treatment of U[N(SiMe$_3$)SiMe$_2$CH$_2$][N(SiMe$_3$)$_2$]$_2$ afforded U(SMes*)[N(SiMe$_3$)$_2$]$_3$ (**2**) and U(SMes*)$_3$-[N(SiMe$_3$)$_2$]. The first neutral homoleptic uranium(IV) thiolate to have been crystallographically characterized, U(SMes*)$_4$ (**4**), was isolated from the reaction of U(BH$_4$)$_4$ and KSMes*. The first homoleptic thiolate complex of uranium(III), U(SMes*)$_3$ (**5**), was synthesized by protonolysis of U[N(SiMe$_3$)$_2$]$_3$ with HSMes* in cyclohexane. The crystal structure of **5** exhibits the novel η^3 ligation mode for the arylthiolate ligand. Comparison of the crystal structure of **5** with those of the isomorphous lanthanide congeners Ln(SMes*)$_3$ (Ln = La, Ce, Pr, and Nd) indicates that the U−S, U−C$_{ipso}$, and U−C$_{ortho}$ bond lengths are shorter than the corresponding ones in the 4f-element analogues, when taking into account the variation in the ionic radii of the metals. The distance between the uranium and the carbon atoms involved in the U···H−C ϵ agostic interaction of each thiolate ligand is shorter, by ∼0.05 Å, than that expected from a purely ionic bonding model. The lanthanide(III)/actinide(III) differentiation was analyzed by density functional theory (DFT). The nature of the M−S bond is shown to be ionic strongly polarized at the sulfur for M = U and iono-covalent (i.e. strongly ionic with low orbital interaction), for M = Ln. The strength of the U···H−C ϵ agostic interaction is proposed to be controlled by the maximization of the interaction between U$^+$ and S$^-$ under steric constraints. The η^3 ligation mode of the arylthiolate ligand is also obtained from DFT.

Introduction

The first thiolate complexes of an f-element, U(SEt)$_4$ and U(S^{n}Bu)$_4$, were prepared by Gilman et al. in 1956 by treatment of U(NEt$_2$)$_4$ with the corresponding thiol.[1] These compounds did not receive much attention, until 1990, when Tatsumi, Gilje, et al. isolated the tetrakis dithiolate complex [Li(dme)]$_4$U(edt)$_4$ from the reaction of UCl$_4$ with Li$_2$edt (edt = ethane-1,2-dithiolate) in dimethoxyethane (dme) and characterized it by X-ray diffraction analysis.[2] Since then, other anionic and/or heterobimetallic homoleptic thiolate and dithiolene compounds of uranium(IV) were synthesized.[3−5] It is noteworthy that since the discovery of the pyrophoric powders of U(SEt)$_4$ and U(S^n-Bu)$_4$, which are likely polymeric in the solid state, there has been no report on the structural characterization of any neutral homoleptic uranium(IV) thiolate compound. Meanwhile, a variety of inorganic and organometallic complexes of uranium-(IV) with thiolate[6−10] or dithiolene[11−14] ligands have been prepared, which clearly demonstrate, contrary to previous assumptions, the stability of their U−S bonds and the richness of their coordination chemistry.

[†] CEA Saclay.
[‡] CEA Valrhô.
[§] University of Toulouse.

(1) Jones, R. G.; Karmas, G.; Martin, G. A. J.; Gilman, H. *J. Am. Chem. Soc.* **1956**, *78*, 4285.
(2) Tatsumi, K.; Matsubara, I.; Inoue, Y.; Nakamura, A.; Cramer, R. E.; Tagoshi, G. J.; Golen, J. A.; Gilje, J. W. *Inorg. Chem.* **1990**, *29*, 4928.
(3) Leverd, P. C.; Lance, M.; Nierlich, M.; Vigner, J.; Ephritikhine, M. *J. Chem. Soc., Dalton Trans.* **1994**, 3563.
(4) Leverd, P. C.; Lance, M.; Nierlich, M.; Vigner, J.; Ephritikhine, M. *J. Chem. Soc., Dalton Trans.* **1993**, 2251.
(5) Roger, M.; Arliguie, T.; Thuéry, P.; Fourmigué, M.; Ephritikhine, M. *Inorg. Chem.* **2005**, *44*, 594.
(6) Leverd, P. C.; Arliguie, T.; Lance, M.; Nierlich, M.; Vigner, J.; Ephritikhine, M. *J. Chem. Soc., Dalton Trans.* **1994**, 501.
(7) Leverd, P. C.; Lance, M.; Vigner, J.; Nierlich, M.; Ephritikhine, M. *J. Chem. Soc., Dalton Trans.* **1995**, 237.
(8) Leverd, P. C.; Ephritikhine, M.; Lance, M.; Vigner, J.; Nierlich, M. *J. Organomet. Chem.* **1996**, *507*, 229.
(9) Ventelon, L.; Lescop, C.; Arliguie, T.; Leverd, P. C.; Lance, M.; Nierlich, M.; Ephritikhine, M. *Chem. Commun.* **1999**, 659.
(10) Lescop, C.; Arliguie, T.; Lance, M. Nierlich, M.; Ephritikhine, M. *J. Organomet. Chem.* **1999**, *580*, 137.
(11) Arliguie, T.; Fourmigué, M.; Ephritikhine, M. *Organometallics* **2000**, *19*, 109.
(12) Arliguie, T.; Thuéry, P.; Fourmigué, M.; Ephritikhine, M. *Organometallics* **2003**, *22*, 3000.
(13) Arliguie, T.; Thuéry, P.; Fourmigué, M.; Ephritikhine, M. *Eur. J. Inorg. Chem.* **2004**, 4502.
(14) Roger, M.; Belkhiri, L.; Thuéry, P.; Arliguie, T.; Fourmigué, M.; Boucekkine, A.; Ephritikhine, M. *Organometallics* **2005**, *24*, 4940.

 10.1021/ja0584830 CCC: $33.50

The chemistry of the thiolate complexes of the lanthanide (Ln) elements has also witnessed a major development in the past decade, stimulated by a fundamental interest in the nature of the Ln−S bond and the potential applications of the Ln ions in chalcogenido-based materials.[15] Concerning the neutral Ln(SR)$_3$ compounds, monomeric species exist as Lewis base adducts, with the notable exception of Sm(S-2,4,6-^{t}Bu$_3$C$_6$H$_2$)$_3$ which was isolated in 1992 by Lappert et al. from the reaction of the alkyl precursor Sm[CH(SiMe$_3$)$_2$]$_3$ with the corresponding thiol;[16] the kinetic stability of this unique 3-coordinate homoleptic compound is likely ensured by the bulkiness of the "supermesityl" thiolate ligand SMes*.

By comparison with the thiolate and dithiolene compounds of uranium(IV) and lanthanides(III), such complexes with the uranium atom in the +3 oxidation state proved to be much more difficult to obtain and isolate, and the only examples are organometallics.[14,17,18] In most cases, these complexes were found to be thermally unstable and undergo valence disproportionation reaction[17] or C−H and C−S bond cleavage of the thiolate ligand to give uranium(IV) derivatives.[18]

Besides the synthetic challenge, such uranium(III) compounds are also attractive in view of establishing structural comparisons with their lanthanide(III) counterparts, with the aim of obtaining a better insight into the nature of the metal−ligand bond and the respective role of the 4f and 5f electrons. Such lanthanide(III)/actinide(III) differentiation was first approached with analogous U(III) and Ln(III) complexes containing alkylphosphine, phosphite,[19] and azine ligands;[20−23] the shortening of the U−P and U−N distances relative to the Ln−P and Ln−N distances, which corresponds to the greater stability of the uranium complexes in solution, was attributed to the more covalent character of the actinide−ligand bond. The synthesis of the dithiolene complexes [Cp*$_2$M(dddt)]$^-$ (M = Ce, Nd, U; dddt = 5,6-dihydro-1,4-dithiine-2,3-dithiolate) then permitted comparison for the first time of the structural parameters of analogous lanthanide(III) and actinide(III) compounds with anionic sulfur ligands.[14] X-ray diffraction and density functional theory (DFT) analysis revealed that the shortening of the U−S bonds relative to the Ln−S bonds is indicative of a stronger metal−sulfur interaction in the U(III) complex due to the presence of a covalent contribution to the U−S bonding. Following these investigations, we were interested in homoleptic thiolate compounds of uranium(III) and lanthanides(III). Our first attempts to prepare U(SR)$_3$ complexes with classical thiols or their alkali metal salts were unsuccessful, giving uranium(IV) derivatives as the sole identified products. These difficulties led us to consider the use of the "supermesityl" thiolate ligand to improve kinetic stabilization of the desired compounds, as observed in the case of the aforementioned samarium complex Sm(SMes*)$_3$.[16] Here we report on the synthesis and X-ray crystal structures of U(SMes*)$_4$, U(SMes*)$_3$, and the lanthanide counterparts Ln(SMes*)$_3$ (Ln = La, Ce, Pr, Nd). The U(III) and Ln(III) complexes, in which the thiolate ligands adopt a novel η^3 ligation mode, were found to exhibit significant structural differences, not only in the M−S bond lengths but also, and quite unexpectedly, in the M−C$_{ipso}$ and M−C$_{ortho}$ distances and the M···H−C ϵ agostic interactions. This novel lanthanide(III)/actinide(III) differentiation is discussed in light of theoretical calculations using the Kohn−Sham formalism of DFT including scalar relativistic effects. The complexes have been simplified to allow the theoretical treatment. In the case of the lanthanide compounds, Ln(SR)$_3$ models (Ln = La, Ce, Pr, and Nd) with R = 2-^{t}BuC$_6$H$_4$ have been optimized. Despite our computational efforts, it has not been possible to treat this complex with uranium, and we had to restrict ourselves to the optimization of USR′(SR)$_2$ with R′ = C$_6$H$_5$ and R = 2-^{t}BuC$_6$H$_4$. To the best of our knowledge, this corresponds to one of the largest uranium(III) complexes to have been calculated at this level of theory.[24] The nature of the bonding in all systems has been subjected to natural bonding analysis (NBO).[25]

Experimental Section

All reactions were carried out under argon (<5 ppm oxygen or water) using standard Schlenk-vessel and vacuum-line techniques or in a glovebox. Solvents were dried by standard methods and distilled immediately before use. The ^{1}H NMR spectra were recorded on a Bruker DPX 200 instrument and referenced internally using the residual protio solvent resonances relative to tetramethylsilane (δ 0). Elemental analyses were performed by Analytische Laboratorien at Lindlar (Germany). 1-Br-2,4,6-^{t}Bu$_3$C$_6$H$_2$ and Pr(SO$_3$CF$_3$)$_3$ (Aldrich) were used without purification. U(NEt$_2$)$_4$,[26] U[N(SiMe$_3$)SiMe$_2$CH$_2$][N(SiMe$_3$)$_2$]$_2$,[27] U(BH$_4$)$_4$,[28] U[N(SiMe$_3$)$_2$]$_3$,[29] La[N(SiMe$_3$)$_2$]$_3$,[30] Ce[N(SiMe$_3$)$_2$]$_3$,[31] and Nd[N(SiMe$_3$)$_2$]$_3$[30] were prepared by published methods. KSMes* was prepared by dropwise addition of a THF solution of HSMes* to a suspension of potassium sand in THF; after 12 h at 20 °C, the colorless solution was filtered and evaporated to dryness, leaving a white powder of KSMes* in almost quantitative yield.[32]

Synthesis of HSMes*. The thiol was prepared by a slight modification of the previously described procedure.[33] A flask was charged with 1-Br-2,4,6-^{t}Bu$_3$C$_6$H$_2$ (2.50 g, 6.99 mmol) and Mg (340 mg, 13.98 mmol) in THF (30 mL). The reaction mixture was stirred at 80 °C for 12 h. After filtration, the volume of the THF solution was increased to 100 mL and sulfur (220 mg, 6.86 mmol) was added. The orange solution was stirred at 80 °C for 30 min. A 1 M THF solution of LiAlH$_4$ (5 mL, 5 mmol) was added dropwise, and water was then carefully added dropwise until gas release ceased. After evaporation to dryness, the white residue was extracted in diethyl ether (100 mL). The solution was filtered and evaporated to dryness under vacuum, leaving a white powder; recrystallization from pentane at −60 °C yielded white needles of HSMes* (700 mg, 36%). ^{1}H NMR (200 MHz, benzene-d_6, 23 °C)

(15) Nief, F. *Coord. Chem. Rev.* **1998**, *178*, 13.
(16) Cetinkaya, B.; Hitchcock, P. B.; Lappert, M. F.; Smith, R. G. *J. Chem. Soc., Chem. Commun.* **1992**, 932.
(17) Stults, S. D.; Andersen, R. A.; Zalkin, A. *Organometallics* **1990**, *9*, 1623.
(18) Arliguie, T.; Lescop, C.; Ventelon, L.; Leverd, P. C.; Thuéry, P.; Nierlich, M.; Ephritikhine, M. *Organometallics* **2001**, *20*, 3698.
(19) Brennan, J. G.; Stults, S. D.; Andersen, R. A.; Zalkin, A. *Organometallics* **1988**, *7*, 1329.
(20) Wietzke, R.; Mazzanti, M.; Latour, J. M.; Pécaut, J. *Inorg. Chem.* **1999**, *38*, 3581.
(21) Mehdoui, T.; Berthet, J. C.; Thuéry, P.; Salmon, L.; Rivière, E.; Ephritikhine, M. *Chem. Eur. J.* **2005**, *11*, 6994.
(22) Mehdoui, T.; Berthet, J. C.; Thuéry, P.; Ephritikhine, M. *Dalton Trans.* **2004**, 579.
(23) Berthet, J. C.; Miquel, Y.; Iveson, P. B.; Nierlich, M.; Thuéry, P.; Madic, C.; Ephritikhine, M. *J. Chem. Soc., Dalton Trans.* **2002**, 3265.
(24) Bursten, B.; Strittmatter, R. J. *J. Am. Chem. Soc.* **1987**, *109*, 6606.
(25) Reed, A. E.; Curtiss, L. A.; Weinhold, F. *Chem. Rev.* **1988**, *88*, 899.
(26) Reynolds, J. G.; Zalkin, A.; Templeton, D. H.; Edelstein, N. M.; Templeton, L. K. *Inorg. Chem.* **1976**, *15*, 2498.
(27) Dormond, A.; El Bouadili, A.; Aaliti, A.; Moise, C. *J. Organomet. Chem.* **1985**, 288, C1.
(28) Volkov, V. V.; Myakishev, K. G. *Radiokhimiya* **1980**, *22*, 745.
(29) Avens, L. R.; Bott, S. G.; Clark, D. L.; Sattelberger, A. P.; Watkin, J. G.; Zwick, B. D. *Inorg. Chem.* **1994**, *33*, 2248.
(30) Schuetz, S. A.; Day, V. W.; Sommer, R. D.; Rheingold, A. L.; Belot, J. A. *Inorg. Chem.* **2001**, *40*, 5292.
(31) Hitchcock, P. B.; Hulkes, A. G.; Lappert, M. F.; Li, Z. *Dalton Trans.* **2004**, 129.
(32) Chadwick, S.; Englich, U.; Ruhhlandt-Senge, K.; Watson, C.; Bruce, A. E.; Bruce, M. R. M. *J. Chem. Soc., Dalton Trans.* **2000**, 2167.
(33) Rundel, W. *Chem. Ber.* **1968**, *101*, 2956.

δ 7.56 (s, 2H, *m*-H), 3.43 (s, 1H, SH), 1.61 (s, 18H, *o*-^{t}Bu), 1.30 (s, 9H, *p*-^{t}Bu). Anal. Calcd for $C_{18}H_{30}S$: C, 77.63; H, 10.86; S, 11.51. Found: 77.67; H, 10.85; S, 11.42.

Reaction of $U(NEt_2)_4$ and 3 mol equiv of HSMes*. Crystals of $U(SMes^*)_3(NEt_2)(py)\cdot 0.5py$ (1·0.5py). An NMR tube was charged with $U(NEt_2)_4$ (5.0 mg, 0.010 mmol) and HSMes* (8.0 mg, 0.030 mmol) in THF-d_8 (0.4 mL). After 2 h at 20 °C, the ^{1}H NMR spectrum showed the quantitative formation of $U(SMes^*)_3(NEt_2)(THF)$. ^{1}H NMR (200 MHz, THF-d_8, 23 °C) δ 137.95 (br s, $w_{1/2}$ = 100 Hz, 4H, CH_2), 55.33 (s, 6H, Me), 1.02 (s, 6H, *m*-H), 0.70 (s, 27H, *p*-^{t}Bu), −17.46 (s, 54H, *o*-^{t}Bu). The orange solution was evaporated to dryness, and recrystallization of the residue from pyridine at −25 °C gave orange crystals of **1**·0.5py suitable for X-ray diffraction analysis.

Synthesis of $U(SMes^*)[N(SiMe_3)_2]_3$ (2). A flask was charged with $U[N(SiMe_3)SiMe_2CH_2][N(SiMe_3)_2]_2$ (71.8 mg, 0.10 mmol) and HSMes* (27.8 mg, 0.10 mmol), and toluene (15 mL) was condensed in it. After stirring for 3 h at 20 °C, the orange solution was filtered and evaporated to dryness, giving an orange powder of **2** (95 mg, 95%). ^{1}H NMR (200 MHz, benzene-d_6, 23 °C) δ 4.39 (s, 2H, *m*-H), 0.61 (s, 18H, *o*-^{t}Bu), −0.01 (s, 9H, *p*-^{t}Bu), −5.27 (s, 54H, Me). Anal. Calcd for $C_{36}H_{83}N_3SSi_6U$: C, 43.38; H, 8.39; N, 4.22; S, 3.22. Found: 43.32; H, 8.26; N, 4.11; S, 3.39. Orange crystals of **2** suitable for X-ray diffraction analysis were deposited from a toluene solution.

Reaction of $U[N(SiMe_3)SiMe_2CH_2][N(SiMe_3)_2]_2$ and 3 mol equiv of HSMes*. An NMR tube was charged with $U[N(SiMe_3)SiMe_2CH_2][N(SiMe_3)_2]_2$ (7.0 mg, 0.010 mmol) and HSMes* (8.0 mg, 0.030 mmol) in toluene-d_8 (0.4 mL). After 2 h at 110 °C, the spectrum of the red solution showed the quantitative formation of $U(SMes^*)_3[N(SiMe_3)_2]$. ^{1}H NMR (200 MHz, toluene-d_8, 23 °C) δ 4.58 (s, 6H, *m*-H), 0.85 (s, 54H, *o*-^{t}Bu), −0.47 (s, 27H, *p*-^{t}Bu), −7.66 (s, 18H, Me).

Synthesis of $U(SMes^*)(BH_4)_3$ (3). A flask was charged with $U(BH_4)_4$ (47.0 mg, 0.16 mmol) and KSMes* (50.0 mg, 0.16 mmol), and toluene (15 mL) was condensed in it. After stirring for 1 h at 20 °C, the red solution was filtered and evaporated to dryness, giving a red oil of **3** (72 mg, 81%). ^{1}H NMR (200 MHz, toluene-d_8, 23 °C) δ 105 (br s, $w_{1/2}$ = 700 Hz, 4H, BH_4), −5.77 (s, 9H, *p*-^{t}Bu), −10.43 (s, 18H, *o*-^{t}Bu), −22.25 (s, 2H, *m*-H). Anal. Calcd for $C_{18}H_{41}B_3SU$: C, 38.60; H, 7.38; S, 5.73. Found: 38.86; H, 7.42; S, 5.60.

Synthesis of $U(SMes^*)_4$ (4). A flask was charged with $U(BH_4)_4$ (24.0 mg, 0.081 mmol) and KSMes* (108 mg, 0.341 mmol), and toluene (10 mL) was condensed in it. After stirring for 2 h at 20 °C, the black solution was filtered and evaporated to dryness, giving a black powder of **4** (70 mg, 64%). ^{1}H NMR (200 MHz, toluene-d_8, 23 °C) δ 3.51 (s, 8H, *m*-H), −0.47 (s, 72H, *o*-^{t}Bu), −1.57 (s, 36H, *p*-^{t}Bu). Coalescence of the signals corresponding to the *o*-^{t}Bu groups and aromatic H was observed at −70 °C, but the slow-limit spectrum could not be obtained. Anal. Calcd for $C_{72}H_{116}S_4U$: C, 64.15; H, 8.67; S, 9.52. Found: 64.02; H, 8.64; S, 9.33. Recrystallization from benzene yielded black crystals of **4**·3C_6H_6 suitable for X-ray diffraction analysis.

Synthesis of $U(SMes^*)_3$ (5). A flask was charged with $U[N(SiMe_3)_2]_3$ (104.3 mg, 0.145 mmol) and HSMes* (95.2 mg, 0.342 mmol), and cyclohexane (5 mL) was condensed in it. After stirring for 2 h at 20 °C, the black solution was filtered and evaporated to dryness, giving a black powder of **5** (120 mg, 77%). ^{1}H NMR (200 MHz, benzene-d_6, 23 °C) δ 12.95 (s, 6H, *m*-H), 5.66 (s, 27H, *p*-^{t}Bu), −13.27 (s, 54H, *o*-^{t}Bu). ^{1}H NMR (200 MHz, toluene-d_8, −70 °C) δ 18.56 (s, 6H, *m*-H), 9.37 (s, 27H, *p*-^{t}Bu), −24.79 (s, 54H, *o*-^{t}Bu). Anal. Calcd for $C_{54}H_{87}S_3U$: C, 60.59; H, 8.19; S, 8.99. Found: 60.31; H, 8.07; S, 8.79. Recrystallization from toluene at −25 °C yielded black crystals of **5** suitable for X-ray diffraction analysis.

Synthesis of $La(SMes^*)_3$ (6). A flask was charged with $La[N(SiMe_3)_2]_3$ (30.4 mg, 0.049 mmol) and HSMes* (40.9 mg, 0.147 mmol), and toluene (15 mL) was condensed in it. After stirring for 2 h at 20 °C, the colorless solution was filtered and evaporated to dryness, giving a white powder of **6** (45.7 mg, 96%). ^{1}H NMR (200 MHz, benzene-d_6, 23 °C) δ 7.68 (s, 6H, *m*-H), 1.59 (s, 54H, *o*-^{t}Bu), 1.48 (s, 27H, *p*-^{t}Bu). Anal. Calcd for $C_{54}H_{87}S_3La$: C, 66.77; H, 9.03; S, 9.90. Found: 66.52; H, 8.84; S, 9.75. Recrystallization from toluene at −25 °C yielded colorless crystals of **6** suitable for X-ray diffraction analysis.

Synthesis of $Ce(SMes^*)_3$ (7). A flask was charged with $Ce[N(SiMe_3)_2]_3$ (78.3 mg, 0.126 mmol) and HSMes* (105.1 mg, 0.377 mmol), and cyclohexane (10 mL) was condensed in it. After stirring for 24 h at 20 °C, the yellow solution was filtered and evaporated to dryness, giving a yellow powder of **7** (120 mg, 98%). ^{1}H NMR (200 MHz, benzene-d_6, 23 °C) δ 9.71 (s, 6H, *m*-H), 3.15 (s, 27H, *p*-^{t}Bu), −6.92 (s, 54H, *o*-^{t}Bu). Anal. Calcd for $C_{54}H_{87}S_3Ce$: C, 66.69; H, 9.02; S, 9.89. Found: 66.41; H, 8.85; S, 9.65. Recrystallization from toluene at −25 °C yielded yellow crystals of **7** suitable for X-ray diffraction analysis.

Synthesis of $Pr(SMes^*)_3$ (8). $Pr[N(SiMe_3)_2]_3$ was prepared by treating $Pr(SO_3CF_3)_3$ (787 mg, 1.34 mmol) with $NaN(SiMe_3)_2$ (738 mg, 4.02 mmol) in a mixture of THF (40 mL) and toluene (20 mL). The reaction mixture was stirred at 85 °C for 24 h. After evaporation to dryness, sublimation of the yellow powder (90 °C, 10^{-3} mbar) afforded a green powder of $Pr[N(SiMe_3)_2]_3$ (85 mg, 10%). ^{1}H NMR (200 MHz, benzene-d_6) δ −8.67 (s, Me). A flask was charged with $Pr[N(SiMe_3)_2]_3$ (40.3 mg, 0.065 mmol) and HSMes* (54.5 mg, 0.195 mmol), and toluene (15 mL) was condensed in it. After stirring for 20 h at 20 °C, the pale-green solution was filtered and evaporated to dryness, giving a pale-green powder of **8** (41.6 mg, 66%). ^{1}H NMR (200 MHz, benzene-d_6, 23 °C) δ 13.38 (s, 6H, *m*-H), 6.11 (s, 27H, *p*-^{t}Bu), −20.10 (s, 54H, *o*-^{t}Bu). Anal. Calcd for $C_{54}H_{87}S_3Pr$: C, 66.63; H, 9.01; S, 9.88. Found: 66.34; H, 8.87; S, 9.68. Recrystallization from toluene at −25 °C yielded colorless crystals of **8** suitable for X-ray diffraction analysis.

Synthesis of $Nd(SMes^*)_3$ (9). A flask was charged with $Nd[N(SiMe_3)_2]_3$ (76.9 mg, 0.123 mmol) and HSMes* (102.9 mg, 0.369 mmol), and cyclohexane (10 mL) was condensed in it. After stirring for 3 h at 20 °C, the green solution was filtered and evaporated to dryness, giving a green powder of **9** (115 mg, 96%). ^{1}H NMR (200 MHz, benzene-d_6, 23 °C) δ 12.46 (s, 6H, *m*-H), 5.15 (s, 27H, *p*-^{t}Bu), −12.60 (s, 54H, *o*-^{t}Bu). Anal. Calcd for $C_{54}H_{87}S_3Nd$: C, 66.40; H, 8.98; S, 9.85. Found: 66.13; H, 8.91; S, 9.73. Recrystallization from toluene at −25 °C yielded green crystals of **9** suitable for X-ray diffraction analysis.

Crystallographic Data Collection and Structure Determination. The data were collected on a Nonius Kappa-CCD area detector diffractometer[34] using graphite-monochromated Mo Kα radiation (λ = 0.71073 Å). The crystals were introduced in glass capillaries with a protective "Paratone-N" oil (Hampton Research) coating. The unit cell parameters were determined from 10 frames, and they were then refined on all data. The data (φ and ω scans with 2° steps) were processed with HKL2000.[35] The structures were solved by Patterson map interpretation with SHELXS-97 and subsequent Fourier-difference synthesis and refined by full-matrix least-squares on F^2 with SHELXL-97.[36] Absorption effects were corrected empirically with the DELABS program in PLATON.[37]

Two compounds, **6** and **7**, present an abrupt phase transition with a critical temperature of about 148(2) and 130(2) K, respectively. In both cases, the structure of the high-temperature phase is isomorphous to those of compounds **5**, **8**, and **9**. The structure of **6** at 100 K has also been determined and is given as Supporting Information, but that of **7** could not be solved, possibly due to microscopic twinning. Due to low crystal quality, the structure of **7** at 135 K could not be refined satisfyingly, and all attempts to grow better crystals failed. This is why this structure has not been used for fine geometric comparisons with the other complexes, whereas the structure of **6** at 150 K has been

(34) *Kappa-CCD Software*; Nonius BV: Delft, The Netherlands, 1998.
(35) Otwinowski, Z.; Minor, W. *Methods Enzymol*. **1997**, *276*, 307.
(36) Sheldrick, G. M. *SHELXS-97* and *SHELXL-97*; University of Göttingen: Göttingen, Germany, 1997.
(37) Spek, A. L. *PLATON*; University of Utrecht: Utrecht, The Netherlands, 2000.

Table 1. Crystal Data and Structure Refinement Details

	1·0.5py	**2**	**4**·3C_6H_6	**5**
empirical formula	$C_{65.5}H_{104.5}N_{2.5}S_3U$	$C_{36}H_{83}N_3SSi_6U$	$C_{90}H_{134}S_4U$	$C_{54}H_{87}S_3U$
M (g mol^{-1})	1261.23	996.68	1582.24	1070.45
cryst syst	monoclinic	monoclinic	monoclinic	monoclinic
space group	$C2/c$	$P2_1/n$	$C2/c$	$P2_1/n$
a (Å)	45.505(3)	11.9370(5)	13.9906(8)	10.1653(2)
b (Å)	11.4419(7)	20.7998(7)	32.6564(19)	37.6490(14)
c (Å)	31.3536(19)	19.5467(7)	19.4059(7)	14.3213(6)
β (deg)	129.181(2)	90.212(2)	107.758(3)	100.070(2)
V (Å^3)	12654.1(14)	4853.2(3)	8443.8(8)	5396.5(3)
Z	8	4	4	4
D_{calcd} (g cm^{-3})	1.324	1.364	1.245	1.318
μ(Mo Kα) (mm^{-1})	2.704	3.562	2.063	3.155
F(000)	5240	2048	3320	2204
T (K)	100	100	100	100
reflns collected	80854	103491	26639	30996
indep reflns	12002	9209	7392	9738
obsd reflns [$I > 2\sigma(I)$]	8363	7861	6408	7824
R_{int}	0.124	0.031	0.068	0.055
params refined	678	451	446	574
R1	0.043	0.026	0.034	0.032
wR2	0.107	0.060	0.074	0.067
S	0.991	1.013	1.014	1.033
$\Delta\rho_{min}$ (e Å^{-3})	−1.43	−0.97	−0.77	−0.48
$\Delta\rho_{max}$ (e Å^{-3})	1.44	0.61	0.60	0.53

	6	**7**	**8**	**9**
empirical formula	$C_{54}H_{87}LaS_3$	$C_{54}H_{87}CeS_3$	$C_{54}H_{87}PrS_3$	$C_{54}H_{87}NdS_3$
M (g mol^{-1})	971.33	972.54	973.33	976.66
cryst syst	monoclinic	monoclinic	monoclinic	monoclinic
space group	$P2_1/n$	$P2_1/n$	$P2_1/n$	$P2_1/n$
a (Å)	10.1325(4)	10.1207(5)	10.1384(9)	10.1528(4)
b (Å)	37.693(4)	37.600(2)	37.698(4)	37.6336(17)
c (Å)	14.3913(8)	14.3679(9)	14.3383(11)	14.3232(6)
β (deg)	99.949(3)	100.070(4)	100.008(6)	100.054(3)
V (Å^3)	5413.7(7)	5383.3(5)	5396.7(9)	5388.7(4)
Z	4	4	4	4
D_{calcd} (g cm^{-3})	1.192	1.200	1.198	1.204
μ(Mo Kα) (mm^{-1})	0.936	0.994	1.050	1.111
F(000)	2064	2068	2072	2076
T (K)	150(2)	135(2)	100	100
reflns collected	39216	52363	60778	30900
indep reflns	9114	9380	10224	9174
obsd reflns [$I > 2\sigma(I)$]	7785	4664	5488	7552
R_{int}	0.052	0.122	0.082	0.056
params refined	546	574	574	574
R1	0.073	0.093	0.046	0.033
wR2	0.180	0.255	0.092	0.074
S	1.000	0.978	0.887	1.018
$\Delta\rho_{min}$ (e Å^{-3})	−1.07	−1.22	−1.00	−0.52
$\Delta\rho_{max}$ (e Å^{-3})	2.54	1.72	0.74	0.33

used, notwithstanding the difference in data collection temperature. The hydrogen atoms bound to carbon atoms involved in M···H−C ϵ agostic bonds were found in Fourier-difference maps for compounds **4**·3C_6H_6 and **5**−**9**, and they could even be refined successfully for compounds **5**, **8**, and **9**, with an isotropic displacement parameter equal to 1.5 times that of the parent atom. The agostic bonds involve either one or two protons, with M···H distances in the range ∼2.5−2.9 Å.

Some disorder is present in two compounds. In **1**, a solvent pyridine molecule is disordered around a binary axis, and in **7**, one ^{t}Bu group is rotationally disordered over two positions which were refined with occupancy parameters constrained to sum to unity and some restraints on bond lengths and displacement parameters. Some unresolved disorder is likely to be present in the high-temperature phases of both **6** and **7** and restraints for the displacement parameters of some badly behaving atoms had to be applied; the highest residual electron density peak in **6** is located near atom S(3) and may be indicative of unresolved disorder affecting this atom. In all compounds, all non-hydrogen atoms were refined with anisotropic displacement parameters. The hydrogen atoms were introduced at calculated positions, except for those involved in agostic bonds (see above), and were treated as riding atoms with a displacement parameter equal to 1.2 (CH, CH_2) or 1.5 (CH_3) times that of the parent atom. Crystal data and structure refinement details are given in Table 1. The molecular plots were drawn with SHELXTL.[38]

Computational Details. In previous studies[39−42] we have shown that large-core relativistic effective core potentials (RECPs) optimized by the Stuttgart−Dresden−Bonn group[43−45] are well adapted to the calculations of the geometries of lanthanide complexes, because the 4f electrons do not participate explicitly in the Ln−X bonds. Different

(38) Sheldrick, G. M. *SHELXTL*, Version 5.1; University of Göttingen: Göttingen, Germany, 1999, distributed by Bruker AXS, Madison, WI.
(39) Maron, L.; Eisenstein, O. *J. Phys. Chem. A* **2000**, *104*, 7140.
(40) Maron, L.; Eisenstein, O. *J. Am. Chem. Soc.* **2001**, *123*, 1036.
(41) Maron, L.; Werkema, E. L.; Perrin, L.; Eisenstein, O.; Andersen, R. A. *J. Am. Chem. Soc.* **2005**, *127*, 279.
(42) Werkema, E. L.; Messines, E.; Maron, L.; Perrin, L.; Eisenstein, O.; Andersen, R. A. *J. Am. Chem. Soc.* **2005**, *127*, 7781.
(43) Dolg, M.; Stoll, H.; Savin, A.; Preuss, H. *Theor. Chim. Acta* **1989**, *75*, 173.
(44) Dolg, M.; Fulde, P.; Kuechle, W.; Neumann C.-S.; Stoll, H. *J. Chem. Phys.* **1991**, *94*, 3011.
(45) Dolg, M.; Stoll, H.; Preuss, H. *Theor. Chim. Acta* **1993**, *85*, 441.

RECPs, one per oxidation state (II and III), have been extracted for each lanthanide element. The basis sets adapted to the different RECPs augmented by an *f* polarization function ($\alpha = 1.000$) have been used. Uranium has been represented by a small-core RECP[46] (14 valence electrons) extracted by the Stuttgart−Dresden−Bonn group in combination with the adapted basis set (up to *g* functions). Sulfur has also been represented by an RECP[47] with the associated basis set augmented by a *d* polarization function ($\alpha = 0.390$).[48] Carbon and hydrogen have been represented by an all-electron, double-ζ quality, 6-31G(d,p) basis set.[49] Calculations have been carried out at the DFT(B3PW91) level of theory[50,51] with the Gaussian 98 software.[52] The nature of the extrema (minimum or transition state) has been established with analytical frequencies calculations. The free energy has been calculated at 298 K using the harmonic approximation. The nature of the bonding has been analyzed by using the NBO[25] module of Gaussian 98.

Results and Discussion

The Uranium(IV) Thiolate Compounds. The synthesis of $U(SMes^*)_4$ was first attempted by following the original procedure of Gilman, i.e. treatment of $U(NEt_2)_4$ with the corresponding thiol. In the presence of 3 mol equiv of HSMes*, $U(NEt_2)_4$ was readily transformed in THF at 20 °C into $U(SMes^*)_3(NEt_2)(THF)_x$ in almost quantitative yield, according to eq 1 (NMR experiment);

$$U(NEt_2)_4 + 3\ HSMes^* \rightarrow U(SMes^*)_3(NEt_2)(solv) + 3\ HNEt_2 \quad (1)$$

solv = THF or py (**1**)

after evaporation to dryness, the residue was dissolved in pyridine, and orange crystals of $U(SMes^*)_3(NEt_2)(py)\cdot 0.5py$ (**1**·0.5py) were deposited upon cooling the solution. The same reaction in refluxing THF or toluene with an excess of HSMes* did not perform the metathesis of the fourth diethylamide ligand. This result, however, was not so surprising since similar reaction of $U(NEt_2)_4$ with HO-2,6-^{t}Bu$_2$C$_6$H$_3$ led to the formation of U(O-2,6-^{t}Bu$_2$C$_6$H$_3$)$_3$(NEt$_2$) which was inert in the presence of the phenol.[53] A view of **1** is shown in Figure 1, and selected bond lengths and angles are listed in Table 2.

The uranium atom is found in a very distorted trigonal bipyramidal configuration, at 0.3549(7) Å from the basal plane of the three sulfur atoms, toward the apical NEt_2 group; the other apical position is occupied by a pyridine ligand. The U−S distances average 2.695(18) Å, a value which is identical to that of 2.696(3) Å in U(S-2,6-Me$_2$C$_6$H$_3$)[N(SiMe$_3$)$_2$]$_3$, the only other neutral thiophenolate uranium compound to have been crystallographically characterized thus far.[54] In these two compounds, the U−S−C angles are respectively equal to 123(1)° (mean value) and 114.9(4)°, and are smaller than the U−O−C angles in the phenoxide analogues, 154(7)° (mean value) in U(O-2,6-^{t}Bu$_2$C$_6$H$_3$)$_3$(NEt$_2$)[53] and 158.6(8)° in U(O-2,6-^{t}Bu$_2$C$_6$H$_3$)[N(SiMe$_3$)$_2$]$_3$;[55] this difference is generally attributed to the stronger π bonding between the uranium and the oxygen atoms, whereas recent DFT calculations on Ln(C$_5$H$_5$)$_2$(EPh) complexes (Ln = La, Lu; E = O, S) suggest that the linearity of the Ln−O−C vector arises largely as a result of electrostatic repulsion between the α carbon and the trivalent metal center.[56] The U−N(1) bond length of 2.119(4) Å is slightly shorter than that of 2.162(5) Å in the corresponding triphenoxide amide complex; to the best of our knowledge, these distances are the shortest thus far reported for U−NR$_2$ bonds.[57] The NEt_2 group is distorted so that the C(1) atom approaches the metal center more closely than C(3); the U−N(1)−C(1) and U−N(1)−C(3) angles are equal to 107.8(3)° and 136.0(3)° respectively, and the short U−C(1) contact of 2.922(5) Å indicates the presence of an U···H−C β agostic interaction.[53] The U−N(2) distance of 2.550(4) Å is unexceptional and can be compared with that of 2.56(8) Å in U(S^{i}Pr)$_2$I$_2$(py)$_3$.[7]

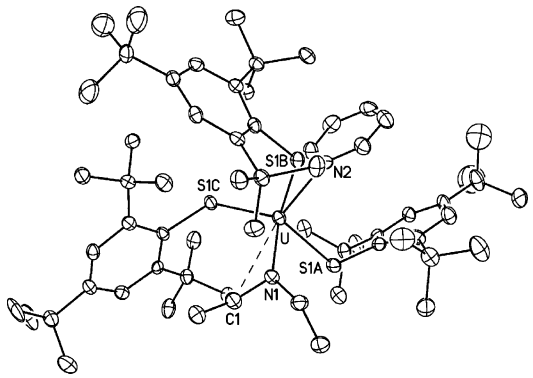

Figure 1. Displacement ellipsoid plot of $U(SMes^*)_3(NEt_2)(py)$ (**1**) drawn at the 30% probability level. The hydrogen atoms and the solvent molecule are omitted. The interaction between the metal and the carbon atom involved in the agostic bond is shown as a dashed line.

Table 2. Selected Bond Lengths (Å) and Angles (deg) for $U(SMes^*)_3(NEt_2)(py)\cdot 0.5Py$ (**1**·0.5py)

U−S(1A)	2.7174(13)	U−S(1A)−C(1A)	123.61(17)
U−S(1B)	2.6937(13)	U−S(1B)−C(1B)	124.55(16)
U−S(1C)	2.6733(13)	U−S(1C)−C(1C)	121.85(16)
U−N(1)	2.119(4)	S(1A)−U−S(1B)	128.76(4)
U−N(2)	2.550(4)	S(1A)−U−S(1C)	108.14(4)
U−C(1)	2.922(5)	S(1B)−U−S(1C)	117.87(4)

The observation that treatment of U[N(SiMe$_3$)SiMe$_2$CH$_2$][N(SiMe$_3$)$_2$]$_2$ with the disubstituted phenol afforded the tetraphenoxide U(O-2,6-^{t}Bu$_2$C$_6$H$_3$)$_4$ led Clark et al. to examine the reactions between the uranium metallacycle and 2,6-disubstituted arenethiols in an attempt to prepare homoleptic uranium(IV) thiolate compounds.[54] However, they found that reaction with 4 mol equiv of HS-2,6-Me$_2$C$_6$H$_3$ yielded highly insoluble, intractable products, presumably uranium sulfides. In contrast, treatment of U[N(SiMe$_3$)SiMe$_2$CH$_2$][N(SiMe$_3$)$_2$]$_2$ with a large excess of HSMes* in refluxing toluene gave a red solution of U(SMes*)$_3$[N(SiMe$_3$)$_2$], whereas the homoleptic tetrathiolate $U(SMes^*)_4$ was not detected (NMR experiments). In the presence of 1 mol equivalent of HSMes*, the metallacycle was readily converted at room temperature into

(46) Kuechle, W. To be published.
(47) Bergner, A.; Dolg, M.; Kuechle, W.; Stoll, H.; Preuss, H. *Mol. Phys.* **1993**, *80*, 1431.
(48) Ehlers, A. W.; Böhme, M.; Dapprich, S.; Gobbi, A.; Höllwarth, A.; Jonas, V.; Köhler, K. F.; Stegmann, R.; Veldkamp, A.; Frenking G. *Chem. Phys. Lett.* **1993**, *208*, 111.
(49) Hariharan, P. C.; Pople, J. A. *Theor. Chim. Acta* **1973**, *28*, 213.
(50) Becke, A. D. *J. Chem. Phys.* **1993**, *98*, 5648.
(51) Burke, K.; Perdew, J. P.; Yang, W. In *Electronic Density Functional Theory: Recent Progress and New Directions*; Dobson, J. F., Vignale, G. Das, M. P., Eds.; Plenum Press: New York, 1998.
(52) Frisch, M. J.; et al. *Gaussian 98*, revision A.9; Gaussian, Inc.: Pittsburgh, PA, 1998.
(53) Van Der Sluys, W. G.; Sattelberger, A. P.; Streib, W. E.; Huffman, J. C. *Polyhedron* **1989**, *8*, 1247.
(54) Clark, D. L.; Miller, M. M.; Watkin, J. G. *Inorg. Chem.* **1993**, *32*, 772.
(55) Berg, J. M.; Clark, D. L.; Huffman, J. C.; Morris, D. E.; Sattelberger, A. P.; Strieb, W. E.; Van Der Sluys, W. G.; Watkin, J. G. *J. Am. Chem. Soc.* **1992**, *114*, 10811.
(56) Russo, M. R.; Kaltsoyannis, N.; Sella, A. *Chem. Commun.* **2002**, 2458.
(57) Berthet, J. C.; Ephritikhine, M. *Coord. Chem. Rev.* **1998**, *178−180*, 83.

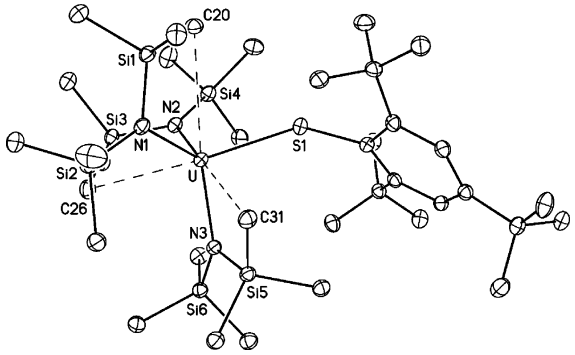

Figure 2. Displacement ellipsoid plot of U(SMes*)[N(SiMe$_3$)$_2$]$_3$ (**2**) drawn at the 30% probability level. The hydrogen atoms are omitted. The interactions between the metal and the carbon atoms involved in the agostic bonds are shown as dashed lines.

Table 3. Selected Bond Lengths (Å) and Angles (deg) for U(SMes*)[N(SiMe$_3$)$_2$]$_3$ (**2**)

U−S(1)	2.6596(8)	U−S(1)−C(1)	139.85(10)
U−N(1)	2.278(2)	S(1)−U−N(1)	120.38(7)
U−N(2)	2.268(2)	S(1)−U−N(2)	96.85(7)
U−N(3)	2.250(2)	S(1)−U−N(3)	100.00(7)
U−C(20)	3.368(3)	N(1)−U−N(2)	106.01(8)
U−C(26)	3.227(3)	N(1)−U−N(3)	117.92(9)
U−C(31)	3.169(3)	N(2)−U−N(3)	114.09(8)

U(SMes*)[N(SiMe$_3$)$_2$]$_3$ (**2**) which was isolated as orange crystals in 95% yield, eq 2.

$$\mathrm{U[N(SiMe_3)SiMe_2CH_2][N(SiMe_3)_2]_2 + HSMes^* \rightarrow U(SMes^*)[N(SiMe_3)_2]_3} \quad (2)$$
(**2**)

The molecular structure of **2** (Figure 2 and Table 3) is very similar to that of U(S-2,6-Me$_2$C$_6$H$_3$)[N(SiMe$_3$)$_2$]$_3$,[54] as shown by the comparison of the U−S distances of 2.6596(8) and 2.696(3) Å, and the average U−N distances of 2.265(12) and 2.24(1) Å, respectively; the steric effect of the bulky ^{t}Bu substituents in **2** clearly manifests itself only in the larger U−S−C angle, 139.85(10)° vs 114.9(4)°. In both compounds, one SiMe$_3$ group of each silylamide ligand is closer to the metal center than the other; in **2**, the short contacts between the uranium and carbon atoms C(20), C(26), and C(31) (Table 3) reflect the presence of U···H−C γ agostic interactions.

The failure to obtain the desired U(SMes*)$_4$ compound by protonolysis of amide precursors led us to consider the metathesis reaction of U(BH$_4$)$_4$ with the alkali metal salt of the thiolate ligand; this route was successful for the synthesis of the anionic homoleptic hexathiolates [Na(THF)$_3$]$_2$U(SR)$_6$ (R = tBu or Ph).[4] Treatment of U(BH$_4$)$_4$ with 1 mol equiv of KSMes* in toluene at 20 °C readily afforded the monothiolate compound U(SMes*)(BH$_4$)$_3$ (**3**), according to eq 3;

$$\mathrm{U(BH_4)_4 + KSMes^* \rightarrow U(SMes^*)(BH_4)_3 + KBH_4} \quad (3)$$
(**3**)

after filtration and evaporation of the solution, the red oil of **3** was recovered in 81% yield. Compound **3** is a unique example of a mixed thiolate/borohydride metal complex, while a series of mixed alkoxide/borohydride derivatives U(OR)(BH$_4$)$_3$(THF)$_2$ and U(OR)$_2$(BH$_4$)$_2$(THF)$_2$ (R = ^{i}Pr, Cy, CHPh$_2$) were synthesized by treating U(BH$_4$)$_4$ with acetone, cyclohexanone, and benzophenone.[58] Addition of more than 1 mol equiv of KSMes* into the toluene solution of U(BH$_4$)$_4$ led to the exclusive formation of the tetrathiolate U(SMes*)$_4$ (**4**); the intermediates U(SMes*)$_n$(BH$_4$)$_{4-n}$ (n = 2, 3) were not detected by ^{1}H NMR spectroscopy. By using the correct stoichiometry and after usual workup, **4** was isolated as a black powder in 64% yield, eq 4;

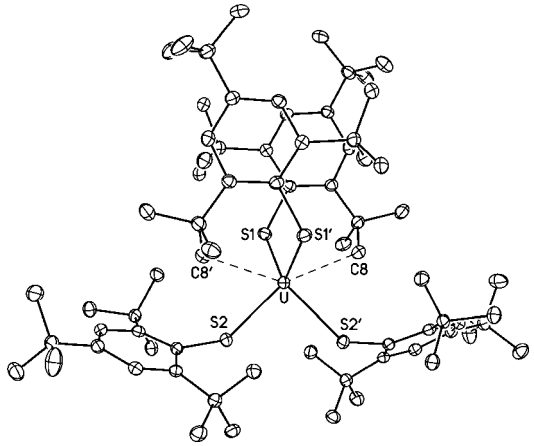

Figure 3. Displacement ellipsoid plot of U(SMes*)$_4$ (**4**) drawn at the 30% probability level. The hydrogen atoms and the solvent molecules are omitted. The interactions between the metal and the carbon atoms involved in the agostic bonds are shown as dashed lines. Symmetry code: ′ = 1 − x, y, $^1/_2$ − z.

Table 4. Selected Bond Lengths (Å) and Angles (deg) for U(SMes*)$_4$·3C$_6$H$_6$ (**4**·3C$_6$H$_6$)

U−S(1)	2.6173(9)	S(1)−U−S(2)	95.87(3)
U−S(2)	2.6294(9)	S(1)−U−S(1′)	109.73(4)
U−C(8)	3.061(4)	S(1)−U−S(2′)	134.41(3)
U−H(8A)	2.65	S(2)−U−S(2′)	91.64(4)
		U−S(1)−C(1)	121.92(12)
		U−S(2)−C(19)	123.17(11)

Symmetry code: ′ = 1−x, y, 1/2−z.

$$\mathrm{U(BH_4)_4 + 4\ KSMes^* \rightarrow U(SMes^*)_4 + 4\ KBH_4} \quad (4)$$
(**4**)

black crystals of **4**·3C$_6$H$_6$ were deposited from a benzene solution. Compound **4** was found to be unstable in THF, giving an insoluble, unidentified yellow precipitate.

Fifty years after Gilman's synthesis of U(SEt)$_4$ and U(S-^{n}Bu)$_4$,[1] **4** is the first neutral homoleptic uranium(IV) thiolate to have been crystallographically characterized. A view of **4** is shown in Figure 3, and selected bond lengths and angles are listed in Table 4.

The uranium atom lies on the C_2 axis, in a distorted tetrahedral environment. The U−S(1) and U−S(2) distances of 2.6173(9) and 2.6294(9) Å seem slightly shorter than those measured in **1** and **2**, and are equal to that of 2.62(2) Å in U(S^{i}Pr)$_2$I$_2$(py)$_3$.[54] The U−S−C angles are similar to those in **1** and are expectedly smaller than the U−O−C angle of 154.0(6)° in the tetraphenoxide U(O-2,6-^{t}Bu$_2$C$_6$H$_3$)$_4$ which exhibits a distinct S_4 symmetry.[53] The lower electron donating capacity of the arylthiolate ligand, by comparison with the related aryloxide group, is compensated by the presence in **4** of an ϵ agostic interaction between the C(8)−H(8A) bond and the metal center, evidenced

(58) Adam, R.; Villiers, C.; Ephritikhine, M.; Lance, M.; Nierlich, M.; Vigner, J. *New J. Chem.* **1993**, *17*, 455.

by the U−C(8) and U−H(8A) distances of 3.061(4) and 2.65 Å, respectively.

The ^{1}H NMR spectra of the complexes indicate that the thiolate, as well as the amide and borohydride ligands are equivalent at 20 °C. Coalescence of the signals of **2** and **4** was observed at lower temperature, but the slow-limit spectra were not attained.

The M(SMes*)$_3$ Complexes (M = U, Nd, Pr, Ce, La). Reactions of $UI_3(THF)_4$ or $U(BH_4)_3(THF)_3$ with KSMes* in THF or treatment of $U(BH_4)_3(THF)_3$ with HSMes* in THF gave intractable products. Eventually, the homoleptic uranium(III) thiolate compound U(SMes*)$_3$ (**5**) was isolated from the protonolysis reaction of the amide precursor $U[N(SiMe_3)_2]_3$ with HSMes* in cyclohexane, as shown by eq 5.

$$U[N(SiMe_3)_2]_3 + 3\ HSMes^* \rightarrow U(SMes^*)_3\ (\mathbf{5}) + 3\ HN(SiMe_3)_2 \quad (5)$$

After 2 h at 20 °C, the solution was filtered and evaporated to dryness, leaving the analytically pure black powder of **5** in 77% yield; dark-brown crystals were deposited from a toluene solution at −25 °C. The synthesis of **5** is similar to that of U(O-2,6-$R_2C_6H_3)_3$ (R = ^{i}Pr, ^{t}Bu) by treatment of $U[N(SiMe_3)_2]_3$ with the corresponding disubstituted phenol.[59] Unlike these phenoxide analogues, **5** was found to be thermally unstable both in the solid state and in solution, being transformed into the uranium(IV) tetrathiolate **4** as the sole detectable product. Solid samples of **5** must be kept below −25 °C to avoid decomposition; in cyclohexane, 50% of **5** was decomposed after 170 h at 23 °C, and **5** was much less stable in toluene, with a half-life of 70 h. For these reasons, it is imperative for the synthesis of **5** to be performed in cyclohexane since, in aromatic solvents, its partial decomposition was observed before complete formation. It is interesting to note that total decomposition of **5** led to the formation of **4** in ∼50% yield, suggesting that the uranium(III) complex underwent the ligand and valence redistribution reaction described by eq 6;

$$2\ U(SMes^*)_3 \rightarrow U(SMes^*)_4 + \text{“}U(SMes^*)_2\text{”} \quad (6)$$

however, the fate of the putative U(SMes*)$_2$ species is unknown. As underlined in the Introduction, the instability of uranium(III) thiolates has already been noticed and is obviously due to the facile $U^{III} \rightarrow U^{IV}$ oxidation. The behavior of **5** is reminiscent of that of the organometallic compound $[(C_5H_4{}^tBu)_2U(SPh)]_2$ which is readily transformed in benzene into $(C_5H_4{}^tBu)_3U(SPh)$ and an unknown subvalent uranium complex.[17]

The crystal structure of **5** is shown in Figure 4, and selected bond lengths and angles are listed in Table 5. The US_3 core exhibits a flattened trigonal pyramidal geometry, the metal center being 0.2991(6) Å from the S_3 plane. The S−U−S angles deviate from 120° by up to 9°, and their sum is equal to 356.4°. This geometry is somewhat different from that of the analogous p-block metal compounds M(SMes*)$_3$ (M = Al, Ga) which adopt a nearly perfect trigonal planar configuration, with the distance between the metal and the S_3 plane equal to 0.09 and 0.08 Å, respectively.[60] The nonplanar, pyramidal geometry of

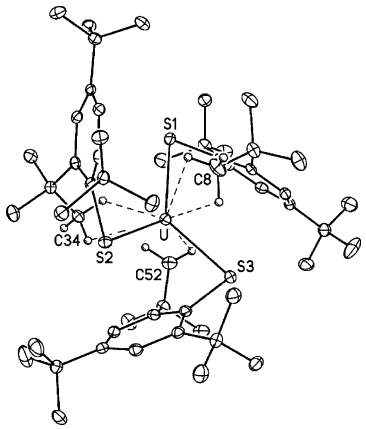

Figure 4. Displacement ellipsoid plot of U(SMes*)$_3$ (**5**) drawn at the 30% probability level. The hydrogen atoms are omitted, except those involved in agostic bonds. The interactions between the metal and these hydrogen atoms are shown as dashed lines. The bonds with C_{ipso} and C_{ortho} atoms are omitted for clarity.

MX_3 complexes has been explained by both electrostatic and covalent models.[61] According to the polarized-ion model, the interligands X···X repulsions become less destabilizing for the larger metal ions, and the pyramidal geometry with X−M−X angles smaller than 120° is less unfavorable; this model also postulates that dipole−dipole attractions increase because of the ease of inducing a dipole moment in the larger metal ions. According to the hybridization model, the stability of the nonplanar configuration is rationalized by the involvement of metal d orbitals in bonding. It is noteworthy that pyramidalization of **5** is much less important than that of the amide and alkyl uranium(III) complexes $U[N(SiMe_3)_2]_3$[61] and $U[CH(SiMe_3)_2]_3$[62] in which the N−U−N and C−U−C angles are 107.7(4) and 116.24(7)°, respectively, and the metal is 0.90 and 0.465(1) Å from the C_3 and N_3 plane, respectively. This difference can be due to the greater steric hindrance of the SMes* ligands and/or the smaller contribution of the metal orbitals to the U−S bonding. The average U−S distance of 2.720(5) Å in **5** is 0.1 Å longer than in **4**, in agreement with the difference in the radii of the U^{III} and U^{IV} ions;[63] it is shorter than the U−S distances in $[Cp^*_2U(SiPr)_2]^-$ [2.78(1) Å][18] and $[Cp^*_2U(dddt)]^-$ [2.773(7) Å],[14] the two other uranium(III) complexes with anionic sulfur ligands to have been crystallographically characterized.

The most salient feature of the structure of **5** is the ligation mode of the thiolate ligand, which is quite different from that in **4**. The U−S−C_{ipso} angles which average 82(4)° are much smaller than in the uranium(IV) thiolates **1** [123(1)°], **2** [139.85(1)°], **4** [122(1)°], and U(S-2,6-$Me_2C_6H_3$)[$N(SiMe_3)_2]_3$ [114.9(4)°],[54] and also in the 3-coordinate compounds M(SMes*)$_3$ [100(3)° for M = Al and Ga].[60] The more acute U−S−C_{ipso} angles bring the C_{ipso} carbon atoms in proximity to the metal center (Table 5); these distances are similar to those measured in U(η^6-C_6Me_6)$(BH_4)_3$ [2.87(2)−2.97(2) Å],[64] the arene-bridged triphenoxide dimer $[U(O\text{-}2,6\text{-}{}^iPr_2C_6H_3)_3]_2$ [2.82(1)−3.02(1) Å][59]

(59) Van Der Sluys, W. G.; Burns, C. J.; Huffman, J. C.; Sattelberger, A. P. *J. Am. Chem. Soc.* **1988**, *110*, 5924.
(60) Ruhlandt-Senge, K.; Power, P. P. *Inorg. Chem.* **1991**, *30*, 2633.
(61) Stewart, J. L.; Andersen, R. A. *Polyhedron* **1998**, *17*, 953.
(62) Van Der Sluys, W. G.; Burns, C. J.; Sattelberger, A. P. *Organometallics* **1989**, *8*, 855.
(63) Shannon, R. D. *Acta Crystallogr., Sect. A* **1976**, *32*, 751.
(64) Baudry, D.; Bulot, E.; Charpin, P.; Ephritikhine, M.; Lance, M.; Nierlich, M.; Vigner, J. *J. Organomet. Chem.* **1989**, *371*, 155.

Table 5. Comparison of Selected Bond Lengths (Å) and Angles (deg) for the Complexes [M(SMes*)$_3$][a]

	M = U (**5**)	M = La (**6**)	M = Ce (**7**)	M = Pr (**8**)	M = Nd (**9**)
M−S(1)	2.7228(10)	2.741(2)	2.703(4)	2.7088(12)	2.6954(8)
M−S(2)	2.7127(11)	2.7599(15)	2.725(3)	2.7108(12)	2.6910(8)
M−S(3)	2.7247(10)	2.759(2)	2.744(4)	2.7197(12)	2.6979(8)
⟨M−S⟩	2.720(5)	2.753(9)	2.724(17)	2.713(5)	2.695(3)
			M−C_{ipso}		
M−C(1)	2.986(4)	3.026(6)	2.998(9)	2.979(4)	2.977(3)
M−C(19)	3.163(4)	3.168(6)	3.122(9)	3.157(4)	3.153(3)
M−C(37)	2.941(4)	2.976(7)	2.962(11)	2.942(4)	2.933(3)
⟨M−C_{ipso}⟩	3.03(10)	3.06(8)	3.03(7)	3.03(9)	3.02(10)
			M−C_{ortho}		
M−C(2)	3.149(4)	3.181(5)	3.172(10)	3.145(4)	3.138(3)
M−C(24)	3.358(4)	3.381(6)	3.365(9)	3.349(4)	3.367(3)
M−C(42)	3.188(4)	3.326(7)	3.360(12)	3.215(4)	3.197(3)
⟨M−C_{ortho}⟩	3.23(9)	3.30(8)	3.30(9)	3.24(8)	3.23(10)
			M−C_{agost}		
M−C(8)	2.933(5)	2.969(12)	2.982(19)	2.929(5)	2.906(4)
M−C(34)	3.036(4)	3.074(6)	3.048(10)	3.048(5)	3.020(4)
M−C(52)	3.198(4)	3.321(10)	3.283(14)	3.216(5)	3.201(4)
⟨M−C_{agost}⟩	3.06(11)	3.12(15)	3.10(13)	3.06(12)	3.04(12)
M−H(8A)	2.62	2.51	2.52	2.58	2.58
M−H(8B)	2.60	2.62	2.65	2.54	2.57
M−H(34A)	2.65	2.52	2.50	2.60	2.64
M−H(34B)	2.65	2.79	2.76	2.69	2.67
M−H(52A)	2.85	2.84	2.81	2.69	2.79
⟨M−H⟩	2.67(9)	2.66(14)	2.65(12)	2.62(6)	2.65(8)
S(1)−M−S(2)	120.38(3)	121.73(6)	122.16(10)	121.10(3)	120.93(2)
S(2)−M−S(3)	111.04(3)	113.59(6)	112.57(10)	111.01(4)	110.79(2)
S(1)−M−S(3)	124.97(3)	123.32(6)	123.83(11)	124.94(4)	125.07(3)
M−S(1)−C(1)	79.99(12)	80.9(2)	80.9(3)	80.16(14)	80.44(10)
M−S(2)−C(19)	86.62(13)	85.59(18)	84.9(3)	86.53(14)	87.13(10)
M−S(3)−C(37)	78.32(12)	78.6(2)	78.6(4)	78.51(13)	78.80(10)

[a] The structures have been determined at −173 °C, excepted those of the La (−123°C) and Ce (−138 °C) compounds.

and Cp*$_2$U(μ-Ph$_2$)BPh$_2$ [2.857(7)−3.166(8) Å];[65] they can also be compared with the average Eu−C and Yb−C distances of 3.065 and 2.973 Å corresponding to η^6-π-arene interactions in the Ln^{II} thiolate complexes Ln(SAr*)$_2$ (Ln = Eu, Yb; Ar* = 2,6-trip$_2$C$_6$H$_3$; trip = 2,4,6-^{i}Pr$_3$C$_6$H$_2$).[66] Moreover, the dihedral angles between the mean plane of the phenyl rings (rms deviation 0.04−0.06 Å) and the plane defined by the U, S, and C_{ipso} atoms deviate from orthogonality by 17−25°, so that one of the two C_{ortho} atoms and its ^{t}Bu substituent are closer to the metal than the others. These geometrical parameters strongly suggest that the SMes* ligand in **5** adopts an η^3 bonding mode involving the S, C_{ipso}, and one of the C_{ortho} atoms; this η^3 ligation mode which, to the best of our knowledge, is unprecedented for the arylthiolate ligand, is reminiscent of that known for some benzyl and arylamide complexes.[67−70] In corroboration of this η^3 coordination of the thiophenolate ligand is the C−C bond length alternation within the aromatic ring, which shows the disruption of aromaticity resulting from the interaction of the C_{ipso}−C_{ortho} bond with the metal center; in Figure 5 are indicated the bond lengths in the USMes* fragment which contains S(1), the same variations can be noted in the other two thiolate ligands. Similar alternation of the aromatic C−C distances was observed in the η^3-arylamide vanadium(III) and titanium(III) compounds V[N(3,5-Me$_2$C$_6$H$_3$)(Ad)]$_3$ (Ad = adamantyl),[68] Ti[N(3,5-Me$_2$C$_6$H$_3$)(^{t}Bu)]$_3$,[69] and Ti[N(3,5-Me$_2$C$_6$H$_3$)(^{t}Bu)]$_2$[CH(SiMe$_3$)$_2$].[70] Like the amide and alkyl compounds U[N(SiMe$_3$)$_2$]$_3$[61] and U[CH(SiMe$_3$)$_2$]$_3$,[62] and also M(SMes*)$_3$ (M = Al, Ga),[60] the uranium(III) thiolate **5** is not lacking in U···H−C agostic interactions. The *ortho* ^{t}Bu substituent on each SMes* ligand which is closer to the uranium atom has one of its methyl groups in short contact with the metal center; this is particularly true for C(8) and C(34), while C(52) is more distant.

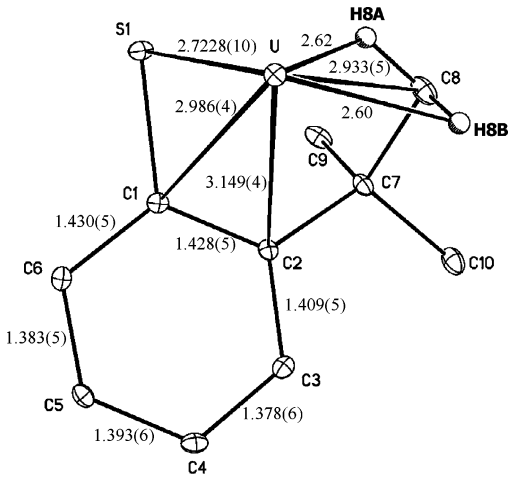

Figure 5. Bond lengths (Å) in one of the three SMes* ligand in **5** (two ^{t}Bu groups have been omitted) showing the η^3 ligation mode of the arylthiolate ligand and the agostic bonds.

(65) Evans, W. J.; Nyce, G. W.; Forrestal, K. J.; Ziller, J. W. *Organometallics* **2002**, *21*, 1050.
(66) Niemeyer, M. *Eur. J. Inorg. Chem.* **2001**, *8*, 1969.
(67) Legzdins, P.; Jones, R. H.; Phillips, E. C.; Yee, V. C.; Trotter, J.; Einstein, F. W. B. *Organometallics* **1991**, *10*, 986 and references herein.
(68) Ruppa, K. B. P.; Desmangles, N.; Gambarotta, S.; Yap, G.; Rheingold, A. L. *Inorg. Chem.* **1997**, *36*, 1194.
(69) Wanandi, P. W.; Davis, W. M.; Cummins, C. C.; Russell, M. A. *J. Am. Chem. Soc.* **1995**, *117*, 2110.
(70) Johnson, A. R.; Davis, W. M.; Cummins, C. C. *Organometallics* **1996**, *15*, 3825.

The U−C_{agost} distances (Table 5) can be compared with those of 3.05 and 3.09 Å in the aforementioned uranium(III) amide and alkyl compounds, while the U−H distances, which vary from 2.60 to 2.85 Å, are close to those found in U[$N(SiMe_3)_2$]$_3$ [2.76−2.84 Å].[61]

Crystals of **5** are isostructural and isomorphous with those of the samarium analogue, which were previously characterized by Lappert et al.; however, the crystal structure of Sm(SMes*)$_3$ is not very accurate.[16] To get meaningful structural comparisons between analogous uranium(III) and lanthanide(III) complexes, the Ln(SMes*)$_3$ complexes [Ln = La (**6**), Ce (**7**), Pr (**8**), and Nd (**9**)] have been synthesized by reaction of Ln[$N(SiMe_3)_2$]$_3$ and 3 mol equiv of HSMes* in toluene (Ln = La and Pr) or cyclohexane (Ln = Ce and Nd); after filtration of the solution and evaporation to dryness, white (Pr, La), yellow (Ce), and green (Nd) analytically pure powders were obtained in good yields. All the complexes crystallized from concentrated toluene solutions at −25 °C. The crystal structures of the neodymium and praseodymium derivatives were determined at −173 °C, as was that of the uranium complex, whereas those of the lanthanum and cerium compounds were determined at −123 and −138 °C, respectively (see Experimental Section). At these temperatures, crystals of M(SMes*)$_3$ (M = La, Ce, Pr, Nd, U) are isomorphous; selected bond lengths and angles are given in Table 5. Variations in the strength of M−X bonds in analogous uranium(III) and lanthanide(III) complexes have been detected through the deviations Δ corresponding to the differences [⟨U−X⟩ − ⟨Ln−X⟩] and [$r(U^{III})$ − $r(Ln^{III})$], $r(M^{III})$ being the ionic radius of the metal.[63] These deviations are generally equal to 0.02−0.05 Å, but are as high as 0.1 Å in the phosphorus complexes $(C_5H_4Me)_3M(L)$ [M = Ce or U; L = PMe_3 or $P(OCH_2)_3CEt$][19] and in the tris(btp) compounds $[M(btp)_3]I_3$ (M = La, Ce, Sm, or U; btp = 2,6-dialkyl-1,2,4-triazin-3-yl)-pyridine),[23] and Δ = 0.2 Å in the terpyridine compounds $[Cp^*_2M(terpy)]I$ (M = Ce, U).[21] These greatest deviations were explained by the softer character and better π-accepting ability of the phosphorus- and nitrogen-containing ligands. Unfortunately, the crystal structure of Ce(SMes*)$_3$ was not determined with a high accuracy (see Experimental Section). Therefore, only the crystal structures of the isomorphous compounds M(SMes*)$_3$ (M = La, Pr, Nd, U) can be compared with good confidence. All the M(SMes*)$_3$ complexes exhibit the novel η^3 coordination of the SMes* ligand and the M···H−C ϵ agostic interactions with one methyl group of an ortho ^{t}Bu substituent on each thiolate ligand. The distances between the metal and the carbon atom involved in the agostic interaction [C_{agost} = C(8), C(34), or C(52)] are ranging between 2.906(4) and 3.321(10) Å, while the corresponding average M−H distances vary from 2.62(6) to 2.72(13) Å. The plots of the M−S, M−C_{ipso}, M−C_{ortho}, and M−C_{agost} distances, for each SMes* ligand of the complexes, as a function of the ionic radii $r(M^{III})$ of the metals are shown in Figures 6−9, respectively, with the regression lines corresponding to the lanthanide derivatives and their r^2 coefficients. The usual linear relationship between the Ln−S or Ln−C distances and $r(Ln^{III})$ is respected, with r^2 coefficients greater than 0.95, except for the regression lines corresponding to the Ln−C_{ortho} and Ln−C_{agost} distances of the thiolate ligand containing S(2). Whatever the M−S or M−C distance in each thiolate group, with the exception of the M−C_{ipso} distances of the thiolate ligand containing S(2), the dots corresponding to the U−S and U−C distances are significantly displaced from the linear plots of the Ln−S and Ln−C distances, and they correspond to values lower than those expected from a purely ionic bonding model. These results strongly suggest that the SMes* ligand has a better affinity for the uranium(III) than for the lanthanide(III) ions, due to the greater strength of both the

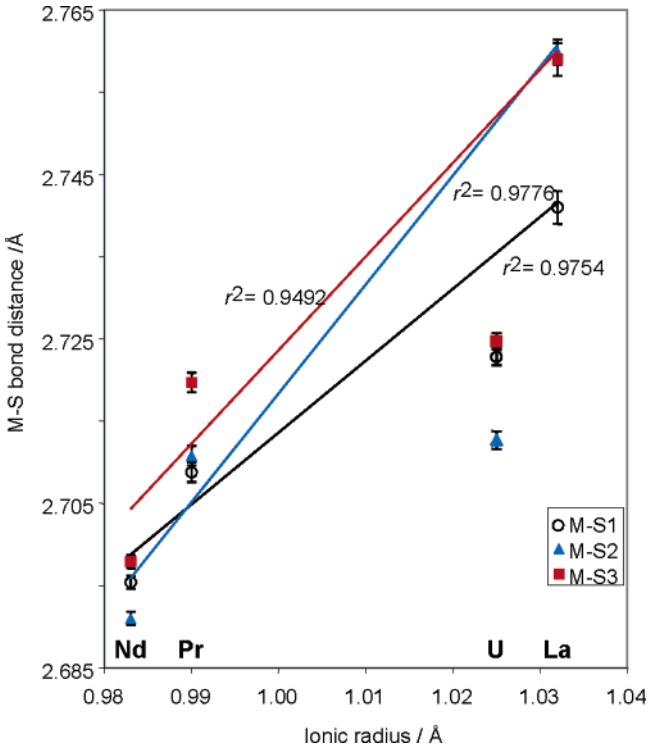

Figure 6. Plot of M−S bond lengths versus metal ionic radii in the isomorphous M(SMes*)$_3$ complexes.

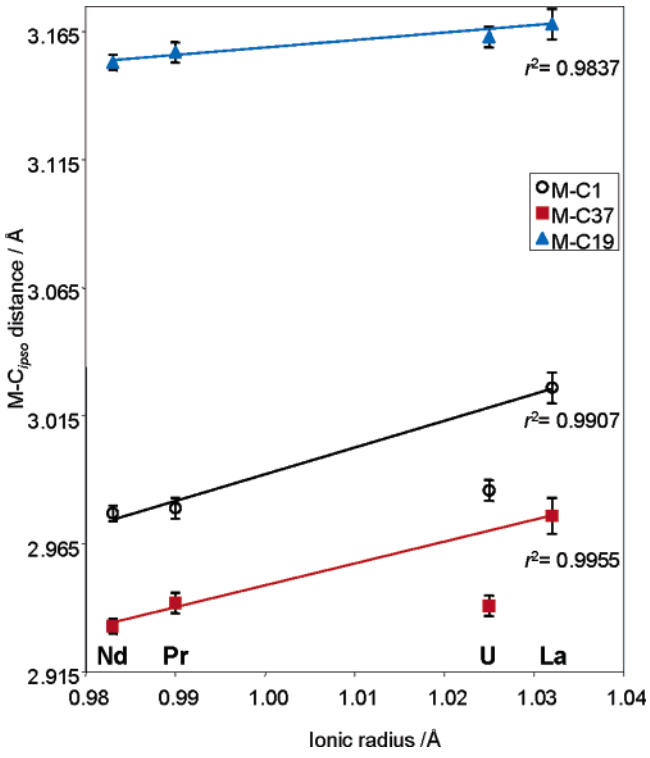

Figure 7. Plot of M−C_{ipso} bond lengths versus metal ionic radii in the isomorphous M(SMes*)$_3$ complexes.

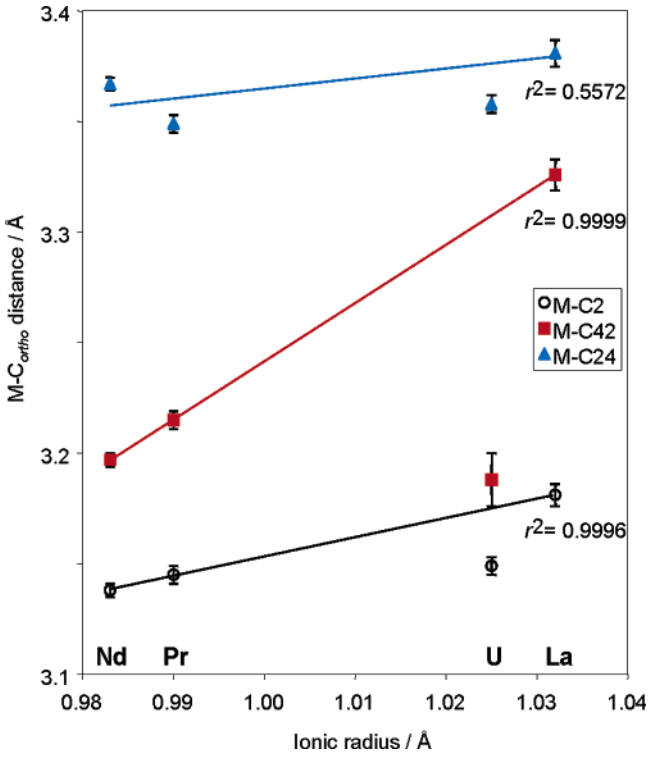

Figure 8. Plot of M−C$_{ortho}$ bond lengths versus metal ionic radii in the isomorphous M(SMes*)$_3$ complexes.

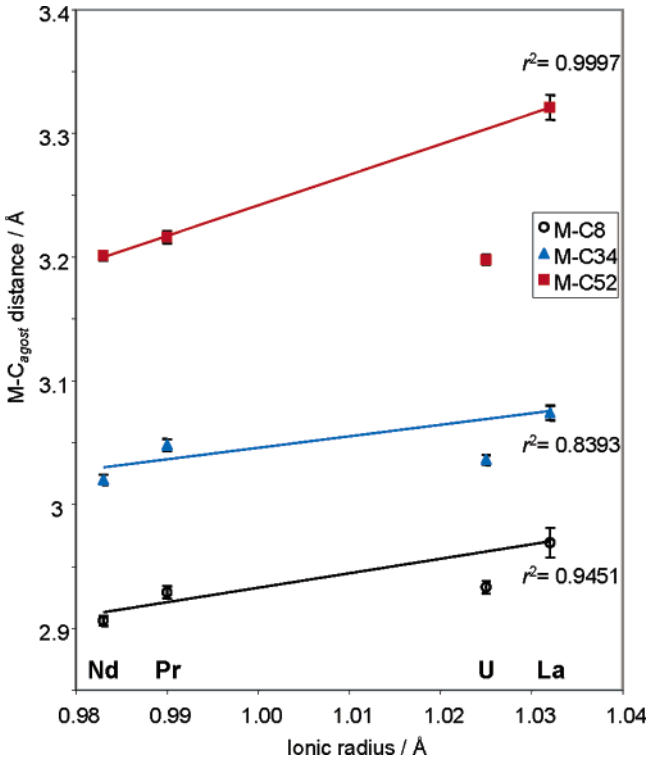

Figure 9. Plot of M−C$_{agost}$ bond lengths versus metal ionic radii in the isomorphous M(SMes*)$_3$ complexes.

η^3 ligation mode of the thiolate group and the U···H−C ϵ agostic interaction.

The shortening of the U−S bonds with respect to the Ln−S bonds, with an average value of 0.025 Å, can be compared with that of 0.03 Å measured in [Cp*$_2$M(dddt)]$^-$ (M = Ce, Nd, U)[14] and [MI$_3$(1,4,7-trithiacyclononane)(MeCN)$_2$] (M = La, U),[71] the only other analogous 4f and 5f-element compounds with a sulfur ligand to have been crystallographically characterized.

The M−C$_{ipso}$ and M−C$_{ortho}$ distances are also shorter in the uranium complex than in the lanthanide analogues by an average value of 0.02 and 0.05 Å, respectively. These differences are similar to those of 0.03 and 0.05 Å between the U−C and Ln−C distances in the series of the trivalent metallocenes (C$_5$H$_4$R)$_3$M(L) (M = Ce, U; R = Me, ^{t}Bu, SiMe$_3$; L = Lewis base)[19,22] and Cp*$_3$M (M = La, Ce, Pr, Nd, Sm, Gd, U),[72,73] respectively; they are also similar to the difference of 0.05 Å between the U−C and Ce−C distances of the N-heterocyclic carbene ligand in Cp*$_2$MI(C$_3$Me$_4$N$_2$) and (C$_5$H$_4$^{t}Bu)$_3$M(C$_3$Me$_4$N$_2$) (M = Ce, U).[74]

While agostic interactions are well documented in f-element chemistry,[61,62,75] the plots of Figure 9, showing that the U−C$_{agost}$ distances are shorter than the Ln−C$_{agost}$ distances by an average value of 0.045 Å, reveal for the first time that such interactions would be stronger in actinide(III) than in lanthanide(III) compounds. A DFT study of the complexes [CpM(PH$_3$)(CH$_2$-CH$_2$)R]$^+$ (M = Co, Rh, Ir; R = H, Me) showed that the strength of the β agostic interaction decreases down the cobalt triad. The M···H−C agostic bond being established by charge donation from the occupied σ_{CH} orbital to an empty d-based orbital on the metal, this trend is in agreement with the fact that cobalt has the more suitable acceptor orbital.[76] By analogy, the stronger agostic interaction in the uranium complex could be due to the easier accessibility of the 5f orbitals. The Ln(III)/An(III) differentiation in the novel η^3 ligation mode of the arylthiolate ligand and the M···H−C ϵ agostic interactions in the isomorphous complexes **5**−**9** were analyzed by density functional theory.

Density Functional Theory Calculations. Relativistic effects are very important for elements as heavy as lanthanides and actinides and have to be accounted for in the calculations.[77] A clever way of taking into account these effects consists of using effective core potentials (ECP) that also reduce the number of electrons to be treated explicitly in the calculations to the valence ones.[78,79] It is also now well-established, both experimentally and theoretically, that 4f electrons do not participate in the bonding[80] whereas the 5f ones, in the case of early actinides, are involved in it.[77,81] This has led some authors to propose the definition of ECPs that include the 4f electrons in core (not treated explicitly) to represent the lanthanide atoms.[43−45] It should be noticed that such an ECP is associated to a given 4f electronic configuration and oxidation state. Using these ECPs allows a DFT treatment of the system since the ground state is considered as a singlet.[39] These ECPs have been successfully used to represent either the geometrical features or the reactivity

(71) Karmazin, L.; Mazzanti, M.; Pécaut, J. *Chem. Commun.* **2002**, 654.
(72) Mehdoui, T.; Berthet, J. C.; Thuéry, P.; Ephritikhine, M. *Dalton Trans.* **2005**, 1263.
(73) Evans, W. J. *Chem Rev.* **2002**, *102*, 2119.
(74) Mehdoui, T.; Berthet, J. C.; Thuéry, P.; Ephritikhine, M. *Chem. Commun.* **2005**, 2860.
(75) Cheng, X.; Lim, S.; Plečnik, C. E.; Liu, S.; Du, B.; Meyers, E. A.; Shore, S. G. *Inorg. Chem.* **2005**, *44*, 6052 and references herein.
(76) Han, Y. Z.; Deng, L. Q.; Ziegler, T. *J. Am. Chem. Soc.* **1997**, *119*, 5939.
(77) Pyykkö, P. *Chem. Rev.* **1988**, *88*, 563.
(78) Durand, Ph.; Barthelat, J. C. *Theor. Chim. Acta*, **1975**, *38*, 283.
(79) Christiansen, P. A.; Lee, Y. S.; Pitzer, K. S. *J. Chem. Phys.* **1979**, *71*, 4445.
(80) Dolg, M.; Stool, H. In *Handbooks on the Physics and Chemistry of Rare Earths*; Gschneidner, K. A., Jr., Eyring L., Eds.; Elsevier Science: Amsterdam, The Netherlands, 1996; Vol. 22, Chapter 152.
(81) Katz, J. J.; Morss, G. T.; Seaborg, L. R. In *The Chemistry of Actinide Elements*; Chapmann and Hall: New York, 1986; Vol. 1.

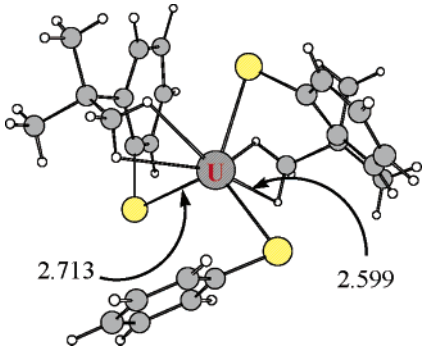

Figure 10. Optimized geometry of $U(SC_6H_5)(S\text{-}2\text{-}^tBuC_6H_4)_2$. U−S and U−H distances in Å.

of lanthanide complexes.[40−42,82] The situation is somehow different in the case of the early actinides, and in particular uranium, since the 5f electrons are chemically active and cannot be included into the core. Small-core ECPs (5f electrons treated explicitly) have also been successfully used in the past to investigate both the structure and the reactivity of uranium (mainly uranyl) complexes in solution.[83,84] In the case of uranium(III) complexes, the number of open f shells (3) should prevent the use of DFT methods since the ground state should be of multiconfigurational character. However, for uranium(IV) complexes, some theoretical investigations have shown that the geometry as well as the vibrational frequencies are correctly reproduced by this method.[83,85] The optimized geometries are presented in Figure 10 for the uranium complex and in Figure 11 for the four lanthanide complexes; selected geometrical parameters are reported in Tables 6 and 7. As mentioned in the Introduction, despite our computational efforts, it has not been possible to optimize the geometry of the $U(SR)_3$ complex with $R = 2\text{-}^tBuC_6H_4$ as for the four lanthanide compounds, and we had to restrict ourselves to the geometry optimization of the complex $USR'(SR)_2$ with $R' = C_6H_5$. This could lead to some difficulties in comparing the theoretically optimized geometry of this complex with those of the lanthanide analogues. Moreover, our theoretical models exhibit only one ^{t}Bu group on the phenyl ring, and that may lead to some discrepancies in the comparison of the experimental and calculated geometrical parameters. Thus, after verifying that the trend obtained theoretically is in agreement with the experimental one, we will analyze the bonding modes in these thiolate complexes, focusing on the M−S bond, the η^3 coordination of the thiolate ligand and the nature of the ϵ-agostic interaction.

The Uranium Complex. As can be seen from Table 6, the geometrical parameters obtained for the calculated uranium complex are in good agreement with the experiment, despite the simplification of the ligand. In particular, it should be noticed that the U−S bonds are well reproduced by the calculations. A NBO analysis of the density does not define any kind of covalent or purely ionic interaction but rather an ionic bond strongly polarized at the sulfur atom, between the positively charged uranium center and the anionic thiolate ligand. The second-order perturbation theory proposed by the NBO analysis clearly indicates some donation from the σ lone pair of sulfur into an empty, mainly f, orbital. However, the donation is calculated to be too small to give rise to an iono-covalent bond, and thus the bonding is better described as an ionic bond strongly polarized at the sulfur atom. On the basis of this bonding mode, it should be noticed that the shorter is the U−S distance the stronger will be this stabilizing interaction.

The η^3 coordination of the thiolate ligand is also correctly reproduced by the calculation (Table 6). Indeed, the very acute $U-S-C_{ipso}$ angle is also found on the optimized geometry leading to a short $U-C_{ipso}$ distance as well as a short $U-C_{ortho}$ distance. This is in agreement with an η^3 coordination mode of the thiolate, which is further confirmed by the C−C distances found in the aromatic ring (Table 7). The experimental distances are nicely reproduced, mainly the $C_{ipso}-C_{ortho}$ one [(C(1)−C(2) in Table 7] despite the simplification of the ligand in the calculation. The NBO analysis gives also indications of an η^3 coordination mode. Indeed, at the second-order perturbation theory, donation from the $C_{ipso}-C_{ortho}$ bond to an empty f orbital of the metal center is observed, indicating an interaction between C_{ortho} and the metal center. Moreover, donation from the $S-C_{ipso}$ bond to an empty f orbital of uranium is also found, showing an interaction between C_{ipso} and the metal center.

The ϵ agostic interaction is also reproduced by the calculation (Table 6 and Figure 10). The shortest U−H and U−S distances are indicated in Figure 10. An idea of the strength of this interaction is obtained by a NBO analysis. Thus, at the second order of perturbation, a donation of a C−H bond of the ^{t}Bu group into an empty d−f hybrid orbital is observed, leading to a stabilization of roughly 5 kcal·mol^{-1}. No evidence for back-donation from the metal center into the σ^* orbital is found.

This agostic interaction is enhanced by a slight hyperconjugation between the aromatic cycle (mainly the $C_{ipso}-C_{ortho}$ bond) and C−C bonds of the ^{t}Bu group, increasing the electron density on this substituent. According to Perrin et al.,[86] an important hyperconjugation of the lone pair of the anion would lead to charge accumulation into the bond trans to the lone pair. Thus, the lone pair is less accessible for interacting with the metal center that moves away from the S_3 plane and this could induce an agostic interaction. However, no hyperconjugation between the lone pairs of the sulfur atom and one C−C bond of the ^{t}Bu group is detected, and thus the presence of the agostic interaction cannot be explained by this phenomenon. This is related to the small pyramidalization found at the uranium center ($\sum S-U-S = 355.39°$). The lack of hyperconjugation is associated with the presence of the aromatic ring that delocalizes more efficiently the lone pairs of the sulfur atom. This is confirmed by NBO analysis at the second-order perturbation, which shows an electronic delocalization between the lone pair of the sulfur atom and the π^* orbital of the $C_{ipso}-C_{ortho}$ bond.

To conclude, the short U−S distance is due to the maximization of the interaction between U^+ and S^- under steric constraints associated to the presence of the ^{t}Bu group. This maximization is the major factor in the formation and strength of the agostic interaction. The U−S bond, described as an ionic bond strongly polarized at the sulfur atom, should be related to the relative softness of the uranium(III) ion, which would allow

(82) Sherer, E. C.; Cramer, C. J. *Organometallics* **2003**, *22*, 1682.
(83) Vallet, V.; Maron, L.; Schimmelpfennig, B.; Leininger, T.; Teichteil, C.; Gropen, O.; Grenthe, I.; Wahlgren, U. *J. Phys. Chem. A* **1999**, *103*, 9285.
(84) Vallet, V.; Schimmelpfennig, B.; Maron, L.; Teichteil, Ch.; Leininger, T.; Gropen, O.; Grenthe, I.; Wahlgren, U. *Chem. Phys.* **1999**, *244*, 185.
(85) Ismail, N.; Heully, J.-L.; Saue, T.; Daudey, J.-P.; Marsden, C. J. *Chem. Phys. Lett.* **1999**, *300*, 296.
(86) Perrin, L.; Maron, L.; Eisenstein, O.; Lappert, M. F. *New J. Chem.* **2003**, *27*, 121.

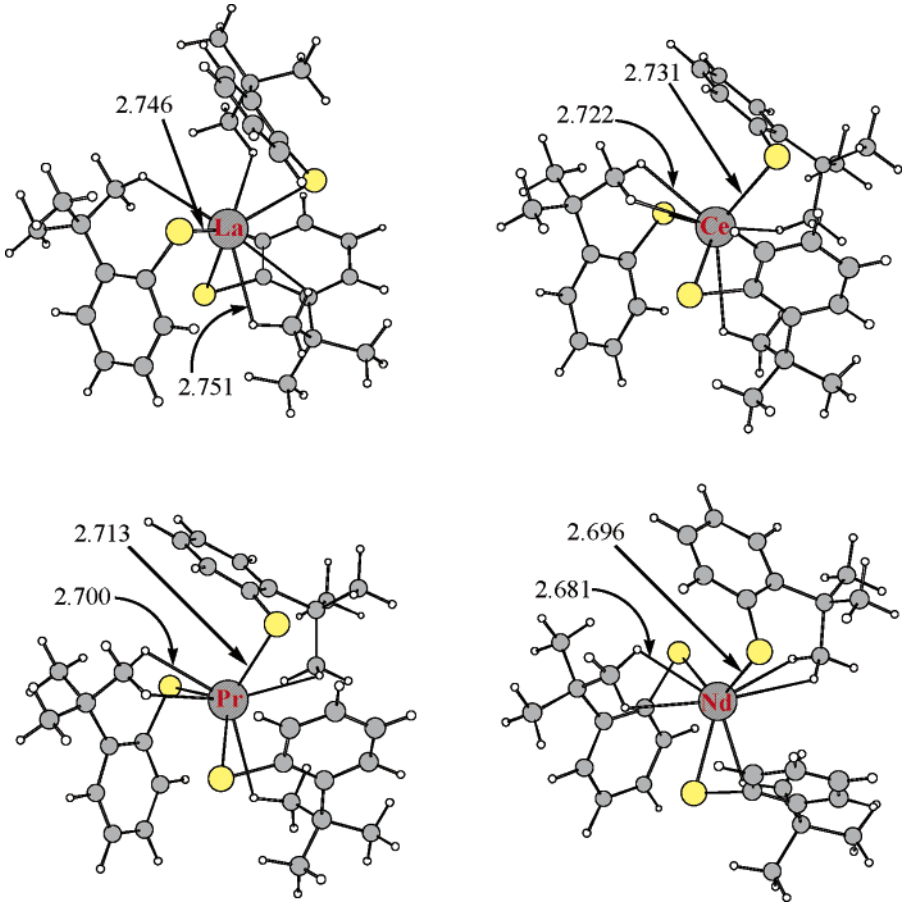

Figure 11. Optimized geometries of Ln(S-2-^{t}BuC$_6$H$_4$)$_3$ (Ln = La, Ce, Pr, Nd). Ln−S and Ln−H distances in Å.

Table 6. Comparison of Selected Bond Lengths (Å) and Angles (deg) for the Calculated Complexes [M(SR)$_3$] with R =2-^{t}BuC$_6$H$_4$

	M = U[a]	M = La	M = Ce	M = Pr	M = Nd
M−S	2.7234	2.7510	2.7312	2.7131	2.6962
	2.7127	2.7598	2.7396	2.7206	2.7035
	2.7246	2.7602	2.7410	2.7228	2.7058
⟨M−S⟩	2.7202	2.7570	2.7372	2.7188	2.7018
M−C$_{ipso}$	2.9867	3.1025	3.1025	3.1056	3.1020
	3.1625	3.0233	3.0083	2.9959	2.9840
	2.9080	3.0798	3.0639	3.0483	3.0378
⟨M−C$_{ipso}$⟩	3.0191	3.0685	3.0582	3.0499	3.0413
M−C$_{ortho}$	3.1498	3.6942	3.6903	3.6913	3.6849
	3.3579	3.6805	3.6719	3.6667	3.6641
	3.3035	3.6226	3.6022	3.5834	3.5711
⟨M−C$_{ortho}$⟩	3.2704	3.6657	3.6548	3.6471	3.6400
M−C$_{agost}$	2.9331	3.3365	3.3073	3.2838	3.2608
	3.0355	3.5198	3.5152	3.5129	3.5207
	n.d	3.2321	3.2031	3.1773	3.1552
⟨M−C$_{agost}$⟩	2.9843	3.3628	3.3418	3.3246	3.3122
S−M−S	120.40	121.69	121.76	121.88	121.87
	111.05	116.20	116.14	116.10	116.20
	124.94	119.78	119.66	119.48	119.36
M−S−C$_{ipso}$	79.99	82.99	83.56	84.20	84.57
	86.60	81.93	81.92	81.88	80.12
	78.29	79.93	79.97	80.06	81.99

[a] The calculations were carried out on USR′(SR)$_2$ with R′ = C$_6$H$_5$ and R = 2-^{t}BuC$_6$H$_4$.

Table 7. Selected Bond Lengths (Å) in the Aromatic Ring for the Calculated Uranium and Neodymium Complexes

uranium complex		neodymium complex	
C(1)−C(2)	1.4276	C(1)−C(2)	1.4256
C(2)−C(3)	1.4081	C(2)−C(3)	1.4053
C(3)−C(4)	1.3779	C(3)−C(4)	1.3915
C(4)−C(5)	1.3925	C(4)−C(5)	1.3901
C(5)−C(6)	1.3829	C(5)−C(6)	1.3884
C(6)−C(1)	1.4298	C(6)−C(1)	1.4096

the delocalization of the sulfur lone pair into the phenyl ring rather than imposing the lone pair to remain in the plane.

The Lanthanide Complexes. As in the uranium case, despite the simplification of the ligand, the main geometrical parameters are correctly reproduced by the calculations (Figure 11 and Table 6). In particular, the η^3 coordination of the thiolate ligand and the presence of a C−H agostic interaction are found in the optimized structures; the shortest Ln−S and Ln−H distances are indicated in Figure 11.

The calculated Ln−S bond lengths are in good agreement with the experimental ones. In particular, the decrease of the Ln−S distances along the series, due to the lanthanide contraction, is found. A NBO analysis of the bonding mode indicates an iono-covalent bond between Ln and S which is confirmed at the second-order perturbation theory. Indeed, a very strong donation of the σ lone pair of sulfur into an empty d orbital is obtained. It should be noted that the interaction no longer originates from the f orbitals but rather from the d ones, in agreement with the absence of any participation of the 4f orbitals in the bonding.[87,88] Moreover, this is also in agreement with

(87) Freedman, D.; Melman, J. H.; Emge, T. J.; Brennan J. G. *Inorg. Chem.* **1998**, *37*, 4162
(88) Lee, J.; Brewer, M.; Berardini, M.; Brennan J. G. *Inorg. Chem.* **1995**, *34*, 3215

the harder character of the Ln(III) ion with respect to uranium(III) one. Indeed, the lone pair of the adjacent sulfur atom remains directed toward the lanthanide ion rather than being delocalized into the phenyl ring.

The η^3 coordination of the thiolate ligand is clearly present in the lanthanide complexes. As seen in Table 6, the acute Ln−S−C_{ipso} angle is reproduced, leading to the short Ln−C_{ortho} and Ln−C_{ipso} distances. As in the uranium complex, an alternation of the C−C bond lengths of the aromatic ring is obtained (Table 7), also in agreement with a η^3 coordination mode of the thiolate ligand. This geometrical feature is confirmed by a NBO analysis. Donation from the C_{ipso}−C_{ortho} bond to an empty d orbital of the metal is found but no evidence of donation from the C_{ipso}−S one to the metal. This is somewhat different from the uranium case and could simply be explained by the fact that the donation from the S lone pair to the metal is more important in the lanthanide complexes than in the uranium analogue. The C_{ipso}−S bond, which is found to be polarized at S (confirmed by NBO analysis), would be less accessible for donation to the metal center since the σ lone pair of the sulfur atom is already interacting with the metal.

The ϵ agostic interaction is also reproduced by the calculation (Table 6 and Figure 11). According to a NBO analysis at the second order of perturbation, a donation of a C−H bond of the ^{t}Bu group into an empty d hybrid orbital is observed, leading to a stabilization of roughly 1 kcal·mol^{-1}. No evidence for back-donation from the metal center into the σ^* orbital is found, in agreement with the nonparticipation of the 4f orbital into the bonding. No hyperconjugation between the aromatic cycle and the C−C bonds of the ^{t}Bu group, that would increase the electron density in the ^{t}Bu group, is observed. In the same way, no hyperconjugation between lone pairs of the sulfur atom and the C−C bonds of ^{t}Bu is detected and consequently, there is no increase in electron density charge on the alkyl substituent. This is in agreement with the small pyramidalization found at the lanthanide centers ($\sum$S−Ln−S = 357.50°). The lack of hyperconjugation is associated, as in the uranium case, with the presence of the aromatic ring that better delocalizes the lone pairs of the sulfur atom. This is confirmed by NBO analysis at the second order of perturbation, which shows an electronic delocalization between the lone pair of the sulfur atom and the π^* orbital of the C_{ipso}−C_{ortho} bond. It should be noticed, however, that this delocalization is found to be less important than that in the uranium case.

Conclusion

The use of the bulky "supermesityl" thiolate ligand SMes* permitted the synthesis of U(SMes*)$_4$, the first neutral homoleptic uranium(IV) thiolate complex characterized by X-ray diffraction analysis, and U(SMes*)$_3$, the first homoleptic thiolate compound of uranium(III). Despite the kinetic stabilization brought by the SMes* ligand, this latter compound was found to decompose at room temperature, both in solution and in the solid sate. The crystal structure of U(SMes*)$_3$ reveals the novel η^3 ligation mode of the arylthiolate ligand and the involvement of a ^{t}Bu substituent on each thiolate group in an U···H−C ϵ agostic interaction. Comparison of the crystal structure of U(SMes*)$_3$ with those of the isomorphous lanthanide congeners Ln(SMes*)$_3$ (Ln = La, Ce, Pr, and Nd) indicates, with the shortening of the U−S and U−C distances with respect to the corresponding ones in the lanthanide analogues, that the η^3 bonding and agostic interaction are stronger in the actinide compound. It should be noted here that the larger strength of the U···H−C versus Ln···H−C agostic interaction could also be assessed by considering the crystal structures of the M[N(SiMe$_3$)$_2$]$_3$ complexes (M = U,[61] Yb,[89] Er,[90] Dy,[90] Eu,[91] Sm,[92] Nd,[93] Ce[94]). Although these structures were not determined under identical experimental conditions, they show that the U−C_{agost} distance is shorter than expected from a purely ionic bonding model. In particular, the average U−C_{agost} distance of 3.047 Å is 0.06 Å shorter than the average Ce−C_{agost} distance, while the ionic radius of uranium(III) is 0.01 Å larger than that of cerium(III). From the DFT perspective, despite the simplification of the ligand, the main geometrical features, especially the M−S distances, are nicely reproduced. The nature of the U−S interaction is found to be an ionic bond strongly polarized at the sulfur atom, whereas the Ln−S bond is essentially ionic. The η^3 ligation mode of the arylthiolate ligand and the M···H−C agostic interaction are also reproduced by the computational calculations. The larger strength of the U···H−C interaction with respect to the Ln···H−C interaction is proposed to be due to the maximization of the U−S interaction under steric constraints, which is confirmed by NBO analysis.

Supporting Information Available: Complete ref 52; Cartesian coordinates of the atoms and absolute energies in hartrees for the optimized geometry complexes; tables of crystal and refinement data, atomic positions and displacement parameters, anisotropic displacement parameters, bond lengths and bond angles in CIF format. This material is available free of charge via the Internet at http://pubs.acs.org.

JA0584830

(89) Niemeyer, M. *Z. Anorg. Allg. Chem.* **2002**, *628*, 647.
(90) Herrmann, W. A.; Anwander, R.; Munck, F. C.; Scherer, W.; Dufaud, V.; Huber, N. W.; Artus, G. R. J. *Z. Naturforsch., B: Chem. Sci.* **1994**, *49*, 1789.
(91) Ghotra, J. S.; Hursthouse, M. B.; Welch, A. J. *J. Chem. Soc., Chem. Commun.* **1973**, 669.
(92) Brady, E. D.; Clark, D. L.; Gordon, J. C.; Hay, P. J.; Keogh, D. W.; Poli, R.; Scott, B. L.; Watkin, J. G. *Inorg. Chem.* **2003**, *42*, 6682.
(93) Andersen, R. A.; Templeton, D. H.; Zalkin, A. *Inorg. Chem.* **1978**, *17*, 2317.
(94) Rees, W. S.; Just, O.; Van Derveer, D. S. *J. Mater. Chem.* **1999**, *9*, 249.